Numer. Math. Theor. Meth. Appl. doi: 10.4208/nmtma.OA-2024-0076

The Direct Discontinuous Galerkin Method with Explicit-Implicit-Null Time Discretizations for Nonlinear Diffusion Equations

Yumiao Li¹, Yin Yang^{2,*}, Tiegang Liu³, Weixiong Yuan³ and Kui Cao³

Received 20 June 2024; Accepted (in revised version) 31 October 2024

Abstract. This paper proposes a discussion of the direct discontinuous Galerkin (DDG) methods coupled with explicit-implicit-null time discretizations (EIN) for solving the nonlinear diffusion equation $u_t = (a(u)u_x)_x$. The basic idea of the EIN method is to add and subtract two equal constant coefficient terms a_1u_{xx} ($a_1 =$ $a_0 \times \max_u a(u)$ on the right-hand side of the above equation, and then apply the explicit-implicit time-marching method to the equivalent equation. The EIN method does not require any nonlinear iterative solver while eliminating the severe timestep restrictions typically associated with explicit methods. We present the stability criterion of the EIN-DDG schemes for the simplified equation with periodic boundary conditions via the Fourier method, where the first order and second order EIN-DDG schemes are unconditionally stable when $a_0 \geq 0.5$ and the third order EIN-DDG scheme is unconditionally stable under the condition $a_0 \geq 0.54$. Numerical experiments show the stability and optimal orders of accuracy of our proposed schemes with a relaxed time-step restriction and the appropriate coefficient a_0 for both linear and nonlinear equations in one-dimensional and two-dimensional settings. Furthermore, we also show that the computational efficiency of our EIN-DDG schemes and explicit Runge-Kutta DDG (EX-RK-DDG) schemes for steady-state equations with small viscosity coefficients to illustrate the effectiveness of the present methods.

AMS subject classifications: 65M60, 65M12, 65M15

Key words: Direct discontinuous Galerkin method, explicit-implicit-null time discretization, stability, nonlinear diffusion equation, steady-state equation.

¹ Hunan International Scientific and Technological Innovation Cooperation Base of Computational Science, Xiangtan University, Xiangtan 411105, China

² National Center for Applied Mathematics in Hunan, Xiangtan University, Xiangtan 411105, China

³ LMIB and School of Mathematical Sciences, Beihang University, Beijing 100191, China

^{*}Corresponding author. Email address: yangyinxtu@xtu.edu.cn (Y. Yang)

1. Introduction

Diffusion is a common phenomenon in nature and has been studied in areas such as percolation, phase change, biochemistry, and population dynamics. It can be effectively modeled using nonlinear diffusion equations. The numerical study of nonlinear diffusion equations has attracted considerable attention from many scholars who are committed to developing higher order numerical methods with stability and convergence.

Although the explicit time-marching method is relatively straightforward to implement, its stability is constrained by the severe time-step $\tau = \mathcal{O}(h^k)$ for the k-th $(k \ge 2)$ order partial differential equations (PDEs), which results in high computational costs and renders the explicit scheme impractical. For example, under a strict CFL-like stability condition $c_0\tau \leq \epsilon \leq c_1h^2$, Liu and Wen [20] proved the third order explicit Runge-Kutta time discretization with the alternating evolution discontinuous Galerkin scheme is stable for linear convection-diffusion equations. The implicit time-marching method can overcome the limitation of a small time-step and can be applied to any order [14]. However, a fully implicit method is not always optimal for solving nonlinear equations, as it necessitates the resolution of a non-symmetric, non-positively deterministic, and nonlinear algebraic system at each time-step [6, 8, 13, 15, 17]. Jay [16] employed the preconditioned linear iterative method to solve approximately the linear systems of the simplified Newton method. However, the above linear system requires computing and storing the Jacobian of nonlinear operators, and its fast solution relies on an efficient preconditioner, which increases the difficulty of the implicit timemarching method. In order to overcome such difficulties, the implicit-explicit (IMEX) time-marching methods [1, 2, 12, 23, 24] have been proposed and treated the higher order derivative terms implicitly and the rest of the terms explicitly. Such a treatment permits a portion of the solution to be explicit, which is typically more efficient than the fully implicit method. Nevertheless, due to each implicit stage requiring solving a nonlinear system, the method may not apply to equations where both the convection and diffusion terms are nonlinear.

To address the abovementioned issues, Douglas and Dupont [7] proposed and adopted a method to guarantee the stability of nonlinear diffusion equations on a rectangular domain. Later, Duchemin and Eggers [9] proposed and referred to that method as explicit-implicit-null method. We take the one-dimensional nonlinear diffusion equation as an example to illustrate the idea of the EIN method. Adding and subtracting the equal term a_1u_{xx} on the right-hand side of the equation $u_t = (a(u)u_x)_x$, we obtain

$$u_t = \underbrace{(a(u)u_x)_x - a_1 u_{xx}}_{T_1} + \underbrace{a_1 u_{xx}}_{T_2}, \quad a_1 = a_0 \times \max_u a(u),$$
 (1.1)

where $a(u) \geq 0$ is bounded and smooth, a_0 is a stabilization parameter and is constant. We treat the term T_1 explicitly and the term T_2 implicitly. Here, the EIN method does not require any nonlinear iterative solver while eliminating the typically severe time-step restrictions, which combines the advantages of both explicit and implicit methods. Recently, the EIN methods coupled with spatial discretizations were success-

fully applied to assure the stability for many problems, such as the two-dimensional radiation hydrodynamics equations with the high order explicit Lagrangian finite volume scheme [18], the convection-diffusion equations and the convection-dispersion equations with spectral collocation schemes [28], the high order dissipative and dispersive equations with the finite difference methods and the LDG methods [27], the nonlinear diffusion equations with the LDG methods [31], the Cahn-Hilliard equations with the LDG methods [25]. For more previous work on the EIN methods, please see [10,11,26,32,39].

However, the LDG method requires complex manipulation of the PDEs, such as introducing auxiliary variables and rewriting the original equations as a first order system, which leads to high computational costs. The DDG method is based on the direct weak formulation for solutions of the equations under consideration, initially proposed by Liu and Yan [21] for linear diffusion equations, without rewriting the equation into a first order system. That method is necessarily identified by an appropriate selection of numerical flux to be used as derivatives of the solution at the cell interface. The numerical flux formula is simple, compact, consistent, and conservative. The most significant features of the DDG method are its low storage requirements and excellent computational performance. In recent studies, the DDG method has been successfully applied to convection-diffusion equations [22, 29, 33], the Korteweg–de Vries equation [36], the Navier-Stokes equation [4,37,38] and compressible turbulent flows [34,35] and so on.

The main purpose of this paper is to develop the DDG method with EIN time-marching method for the nonlinear diffusion equations. By the aid of the Fourier method, we present the first order to third order EIN-DDG schemes and their stability and optimal orders of accuracy under the relaxed time-step restriction and suitable stabilization parameter a_0 . In addition, to demonstrate the advantages of our schemes, we compare the computational efficiency required to reach the steady state for the EX-RK-DDG scheme and the EIN-DDG scheme for convection-diffusion equations with small viscosity coefficients. Although our analysis is based on a one-dimensional diffusion equation, numerical experiments demonstrate that the conclusions can also be extended to the one-dimensional and two-dimensional linear and nonlinear convection-diffusion equations.

The rest of the paper is organized as follows. Section 2 presents the DDG method with the EIN time-marching methods for diffusion equation. Section 3 is devoted to analyzing the stability of the EIN-DDG schemes for the linear diffusion equation via the Fourier method. In Section 4, numerical tests are given to verify the stability, the optimal orders of accuracy, and the computational efficiency of the EIN-DDG schemes for the one-dimensional and two-dimensional linear and nonlinear equations. Finally, the concluding remarks are given in Section 5.

2. The numerical schemes

In this section, we present the discontinuous finite element space and the semidiscrete DDG scheme, and introduce the EIN Runge-Kutta time discretization methods.

For simplicity of analysis, we consider the one-dimensional linear diffusion equation

$$u_t = au_{xx}, \quad x \in \Omega \times (0, T) \tag{2.1}$$

with initial condition $u(x,0) = \sin(\alpha x)$. Similar to the Eq. (1.1), we can obtain the following equivalent form of (2.1):

$$u_t = \underbrace{(a - a_1)u_{xx}}_{T_1} + \underbrace{a_1u_{xx}}_{T_2}, \quad a_1 = a_0 \times a,$$
 (2.2)

where a_0 is the stabilization parameter. We will discretize the term T_1 explicitly and the term T_2 implicitly in (2.2).

2.1. The discontinuous finite element space

Let

$$\mathcal{T}_h = \left\{ I_j = (x_{j-\frac{1}{2}}, x_{j+\frac{1}{2}})_{j=1}^N \right\}$$

be a uniform partition of $\Omega=(x_L,x_R)$, with mesh size $h:=x_{j+1/2}-x_{j-1/2}$, where $x_{1/2}=x_L$ and $x_{N+1/2}=x_R$ are two boundary endpoints. Then, we can define the following discontinuous finite element space:

$$V_h = \{ v \in L^2(I) : v|_{I_i} \in \mathcal{P}_k(I_j), \ \forall j = 1, \dots, N \},$$
(2.3)

where $\mathcal{P}_k(I_j)$ denotes the space of polynomials up to degree k on cell I_j , where k is a non-negative integer. For any $u \in V_h$, there are two traces at an element interface $x_{j+1/2}, \ j=0,\ldots,N$, namely

$$u_{j+\frac{1}{2}}^+ = \lim_{\epsilon \to 0^+} u(x_{j+\frac{1}{2}} + \epsilon), \quad u_{j+\frac{1}{2}}^- = \lim_{\epsilon \to 0^-} u(x_{j+\frac{1}{2}} + \epsilon),$$

and we denote its jump and average as

$$[u]_{j+\frac{1}{2}} = u_{j+\frac{1}{2}}^+ - u_{j+\frac{1}{2}}^-, \quad \{u\}_{j+\frac{1}{2}} = \frac{1}{2} \left(u_{j+\frac{1}{2}}^+ + u_{j+\frac{1}{2}}^- \right).$$

2.2. The spatial discretizations

The semi-discrete DDG scheme of (2.2) is to find the unique approximation solution $u \in V_h$, such that for arbitrary test functions $v \in V_h$, we have

$$(u_t, v)_j = \underbrace{(a - a_1) \left(\widehat{u_x} v\big|_{j - \frac{1}{2}}^{j + \frac{1}{2}} - (u_x, v_x)_j\right)}_{T_t} + \underbrace{a_1 \left(\widehat{u_x} v\big|_{j - \frac{1}{2}}^{j + \frac{1}{2}} - (u_x, v_x)_j\right)}_{T_t}, \tag{2.4}$$

where $(\cdot,\cdot)_j$ denotes the inner product in $L^2(I_j)$, and

$$\widehat{u_x}v\big|_{j-\frac{1}{2}}^{j+\frac{1}{2}} = (\widehat{u_x})_{j+\frac{1}{2}}v_{j+\frac{1}{2}}^- - (\widehat{u_x})_{j-\frac{1}{2}}v_{j-\frac{1}{2}}^+.$$

Here $v_{j\pm 1/2}$ denote values v at $x=x_{j\pm 1/2}$, with the numerical flux term $\widehat{u_x}$ defined as

$$\widehat{u_x} = \frac{\beta_0}{h} [u] + \{u_x\} + \beta_1 h[u_{xx}], \tag{2.5}$$

where β_0 and β_1 are coefficients to be chosen to ensure the stability of the scheme. In our work, we take $\beta_0=1\sim 4$ and $\beta_1=1/12$ according to the work of Liu *et al.* [3, 19, 21]. It is important to note that the above numerical flux is both consistent and conservative, i.e., $\widehat{u_x}=u_x$ for any smooth u and $\widehat{u_x}$ is single-valued.

Remark 2.1. For the nonlinear diffusion equation (1.1), where $w \in V_h$ is taken as the test function, the DDG scheme is defined as follows:

$$(u_{t}, w)_{j} = \underbrace{\left(\widehat{a(u)u_{x}}w\big|_{j-\frac{1}{2}}^{j+\frac{1}{2}} - (a(u)u_{x}, w_{x})_{j}\right) - a_{1}\left(\widehat{u_{x}}w\big|_{j-\frac{1}{2}}^{j+\frac{1}{2}} - (u_{x}, w_{x})_{j}\right)}_{T_{1}} + \underbrace{a_{1}\left(\widehat{u_{x}}w\big|_{j-\frac{1}{2}}^{j+\frac{1}{2}} - (u_{x}, w_{x})_{j}\right)}_{T_{2}},$$

where

$$\widehat{a(u)u_x} = \frac{\beta_0}{h}[b(u)] + \{b(u)_x\} + \beta_1 h [b(u)_{xx}], \quad b(u) = \int_0^u a(s)ds.$$

2.3. The temporal discretizations

This subsection briefly introduces the EIN RK method used in this paper. The semidiscrete DDG scheme can be expressed in the following form:

$$\frac{du}{dt} = \mathcal{L}(t, u) + \mathcal{N}(t, u) =: \mathcal{R}(t, u), \tag{2.6}$$

where $\mathscr{L}(t,u)$ is derived from T_2 in (2.4) and is treated implicitly, whereas $\mathscr{N}(t,u)$ is derived from T_1 in (2.4) and is treated explicitly, and $\mathscr{R}(t,u)$ is the residual. The general s-stage EIN RK time-marching scheme is employed to solve the Eq. (2.2) whose solution advanced from time t^n to $t^{n+1}=t^n+\tau$ is given by

$$u^{n,1} = u^{n},$$

$$u^{n,i} = u^{n} + \tau \sum_{j=1}^{i} a_{ij} \mathcal{L}\left(t_{n}^{j}, u^{n,j}\right) + \tau \sum_{j=1}^{i-1} \hat{a}_{ij} \mathcal{N}\left(t_{n}^{j}, u^{n,j}\right), \quad 2 \leq i \leq s+1,$$

$$u^{n+1} = u^{n} + \tau \sum_{j=1}^{s+1} b_{i} \mathcal{L}\left(t_{n}^{i}, u^{n,i}\right) + \tau \sum_{j=1}^{s+1} \hat{b}_{i} \mathcal{N}\left(t_{n}^{i}, u^{n,i}\right),$$
(2.7)

where τ is the time-step, $u^{n,i}$ denotes the intermediate stages,

$$c_i = \sum_{j=1}^{i} a_{ij} = \sum_{j=1}^{i-1} \hat{a}_{ij}, \quad 2 \leqslant i \leqslant s+1,$$

and $t_n^j = t_n + c_j \tau$. Denote

$$A = (a_{ij}), \quad \hat{A} = (\hat{a}_{ij}) \in \mathbb{R}^{(s+1)\times(s+1)},$$

 $\boldsymbol{b}^{\top} = [b_1, \dots, b_{s+1}], \quad \hat{\boldsymbol{b}}^{\top} = [\hat{b}_1, \dots, \hat{b}_{s+1}], \quad \boldsymbol{c}^{\top} = [0, c_2, \dots, c_{s+1}].$

The general *s*-stage EIN RK scheme can be expressed as the Butcher tableau as follows:

$$\begin{array}{c|c} \boldsymbol{c} & A & \hat{A} \\ \hline & \boldsymbol{b}^\top & \hat{\boldsymbol{b}}^\top \end{array}.$$

In this paper, we consider the following three specific EIN RK time discretizations:

- First order EIN RK scheme in [1]:

- Second order EIN RK scheme in [31]:

- Third order EIN RK scheme in [1]:

The second order EIN RK scheme (2.9) we consider is a modification of the second order scheme given by [5]

where $\mu \neq 0$. Note, at the first stage, the discretization of $\mathcal{L}(t,u)$ in (2.9) is implicit, whereas scheme (2.11) discretizes $\mathcal{L}(t,u)$ explicitly, thus the stability of the scheme (2.9) is better than that of the scheme (2.11). In addition, the third order EIN RK scheme (2.10) is a four-stage, third order, L-stable, singly diagonally implicit RK method, coupled with a four-stage, third order explicit RK method. For more detailed time discretization methods, please see [1,2].

3. Stability analysis

In this section, we use the standard Fourier analysis to analyze the stability of the proposed EIN-DDG schemes. We would like to investigate how to choose a_0 so that the EIN-DDG schemes are unconditionally stable.

Given that we have performed explicit and implicit treatments of the two equal terms in Eq. (2.2), it can be concluded that a larger a_0 would lead to more significant errors. However, a minimal value of a_0 cannot be used to maintain the proposed scheme's stability. Thus, our study's objective is to investigate the threshold value of parameter a_0 that ensures the stability of our EIN-DDG schemes. Since the L^2 -norm of the exact solution to the Eq. (2.1) does not increase in time, we can obtain the stability condition of the EIN-DDG scheme in the following lemma [27].

Lemma 3.1. If G is uniformly diagonalizable and $|\lambda_G| \leq 1$ holds for all $\xi = \alpha h \in [-\pi, \pi]$, where λ_G is the spectral radius of G, then the EIN-DDG scheme is stable.

3.1. First order EIN-DDG scheme

Now, with the aid of the Fourier method, we give the stability result of the first order EIN-DDG scheme in the following theorem.

Theorem 3.1. If $a_0 \ge 0.5$, then the first order EIN-DDG scheme is unconditionally stable.

Proof. By choosing the Lagrangian polynomial $L_j(x)=1$ as the basis function, we can express the numerical solution as $u(x,t)|_{I_j}=u_jL_j(x),\ 1\leq j\leq N.$ Taking v=1 in (2.4), we have

$$(u_j)_t = \frac{1}{h^2} \left((a - a_1)(\beta_0 u_{j-1} - 2\beta_0 u_j + \beta_0 u_{j+1}) + a_1(\beta_0 u_{j-1} - 2\beta_0 u_j + \beta_0 u_{j+1}) \right).$$
 (3.1)

Note, when k=0, the numerical flux (2.5) reduces to $\widehat{u_x}=\beta_0[u]/h$.

We make an ansatz of the form $u_j = \hat{u}_j e^{i\alpha x_j}$, $i^2 = -1$, and substitute this into (3.1), then obtain

$$(\hat{u}_j)_t = \frac{1}{h^2} \left((a - a_1)(\beta_0 e^{-i\alpha h} - 2\beta_0 + \beta_0 e^{i\alpha h}) + a_1(\beta_0 e^{-i\alpha h} - 2\beta_0 + \beta_0 e^{i\alpha h}) \right) \hat{u}_j.$$
 (3.2)

When this equality is combined with the EIN time discretization (2.8), it gives

$$\hat{u}_j^{n+1} = G\hat{u}_j^n,$$

where G is given by

$$G = 1 + 2\beta_0 (1 - a_0) a\lambda(\cos \xi - 1) + 2\beta_0 a_0 a\lambda(\cos \xi - 1) \frac{1 + 2\beta_0 (1 - a_0) a\lambda(\cos \xi - 1)}{1 - 2\beta_0 a_0 a\lambda(\cos \xi - 1)} = 1 + \frac{2\beta_0 a\lambda(\cos \xi - 1)}{1 - 2\beta_0 a_0 a\lambda(\cos \xi - 1)},$$
(3.3)

and $\lambda = \tau/h^2$. By applying Lemma 3.1, we have

$$\left| 1 + \frac{2\beta_0 a\lambda(\cos\xi - 1)}{1 - 2\beta_0 a_0 a\lambda(\cos\xi - 1)} \right| \le 1,\tag{3.4}$$

i.e.,

$$\begin{cases} a_0 > \frac{1}{2\beta_0 a\lambda(\cos \xi - 1)}, \\ (2a_0 - 1)\beta_0 a\lambda(\cos \xi - 1) \le 1, \\ 2\beta_0 a\lambda(\cos \xi - 1) \le 0. \end{cases}$$

Then we can conclude that $a_0 \ge 0.5$. So, we completed the proof of this theorem. \Box

3.2. Second order and third order EIN-DDG schemes

In this subsection, taking the third order EIN-DDG scheme as an example, we can also use the Fourier analysis to obtain the stability result.

Similarly, we define the Lagrangian nodal basis polynomials as

$$L_j^s(x) = \prod_{\substack{l=0\\l \neq s}}^2 \frac{(x - x_j^l)}{(x_j^s - x_j^l)}, \quad 0 \le s \le 2, \quad 1 \le j \le N,$$

where the grid points are defined as $x_j^s = x_j + ((s-1)/3)h$, and the numerical solution u(x,t) inside each cell I_j can be represented as

$$u(x,t)|_{I_j} = \sum_{l=0}^{2} u_j^l(t) L_j^l(x).$$

Here we choose the point values of the solution $u(x_j^s,t)$ inside cell I_j as the degree of freedom, denoted by $u_i^s(t), \ 0 \le s \le 2, \ 1 \le j \le N$.

By taking the test functions v as $L_j^s(x)$, $0 \le s \le 2$, $1 \le j \le N$, and inverting the small 3×3 mass matrix, we can rewrite the DDG scheme (2.4) as

$$(\mathbf{u}_j)_t = \frac{1}{h^2} ((a - a_1)(A\mathbf{u}_{j-1} + B\mathbf{u}_j + C\mathbf{u}_{j+1}) + a_1(A\mathbf{u}_{j-1} + B\mathbf{u}_j + C\mathbf{u}_{j+1})), \quad (3.5)$$

where $\mathbf{u}_j = (u_i^0(t), u_i^1(t), u_i^2(t))^{\top}$ and the specific form of the matrices defined as

$$A = \begin{pmatrix} a_{11} & a_{12} & a_{13} \\ a_{21} & a_{22} & a_{23} \\ a_{31} & a_{32} & a_{33} \end{pmatrix}, \quad B = \begin{pmatrix} b_{11} & b_{12} & b_{13} \\ b_{21} & b_{22} & b_{23} \\ b_{31} & b_{32} & b_{33} \end{pmatrix}, \quad C = \begin{pmatrix} c_{11} & c_{12} & c_{13} \\ c_{21} & c_{22} & c_{23} \\ c_{31} & c_{32} & c_{33} \end{pmatrix},$$

$$a_{11} = \frac{23}{16} \left(-4 + \beta_0 + 24\beta_1 \right), \qquad a_{12} = \frac{1}{24} \left(414 - 115\beta_0 - 1656\beta_1 \right),$$

$$a_{13} = \frac{1}{16} \left(-184 + 115\beta_0 + 552\beta_1 \right), \quad a_{21} = \frac{9}{16} \left(4 - \beta_0 - 24\beta_1 \right),$$

$$a_{22} = \frac{3}{8} \left(-18 + 5\beta_0 + 72\beta_1 \right), \qquad a_{23} = \frac{9}{16} \left(8 - 5\beta_0 - 24\beta_1 \right),$$

$$a_{31} = \frac{1}{16} \left(16 - \beta_0 - 24\beta_1 \right), \qquad a_{32} = \frac{1}{24} \left(-18 + 5\beta_0 + 72\beta_1 \right),$$

$$a_{33} = \frac{1}{16} \left(8 - 5\beta_0 - 24\beta_1 \right), \qquad b_{11} = \frac{3}{8} \left(-6 - 19\beta_0 - 88\beta_1 \right),$$

$$b_{12} = \frac{1}{12} \left(-18 + 55\beta_0 + 792\beta_1 \right), \qquad b_{13} = \frac{3}{8} \left(10 - 3\beta_0 - 88\beta_1 \right),$$

$$b_{21} = \frac{3}{8} \left(42 + 9\beta_0 + 72\beta_1 \right), \qquad b_{22} = \frac{3}{4} \left(-42 - 5\beta_0 - 72\beta_1 \right),$$

$$b_{23} = \frac{9}{8} \left(14 + 3\beta_0 + 24\beta_1 \right), \qquad b_{31} = \frac{3}{8} \left(10 - 3\beta_0 - 88\beta_1 \right),$$

$$c_{11} = \frac{1}{16} \left(8 - 5\beta_0 - 24\beta_1 \right), \qquad c_{12} = \frac{1}{24} \left(-18 + 5\beta_0 + 72\beta_1 \right),$$

$$c_{13} = \frac{1}{16} \left(16 - \beta_0 - 24\beta_1 \right), \qquad c_{21} = \frac{9}{16} \left(8 - 5\beta_0 - 24\beta_1 \right),$$

$$c_{22} = \frac{3}{8} \left(-18 + 5\beta_0 + 72\beta_1 \right), \qquad c_{23} = \frac{9}{16} \left(4 - \beta_0 - 24\beta_1 \right),$$

$$c_{24} = \frac{3}{16} \left(-184 + 115\beta_0 + 552\beta_1 \right), \qquad c_{32} = \frac{1}{24} \left(414 - 115\beta_0 - 1656\beta_1 \right),$$

$$c_{33} = \frac{23}{16} \left(-4 + \beta_0 + 24\beta_1 \right).$$

We make an ansatz of the form

$$\begin{pmatrix} u_j^0(t) \\ u_j^1(t) \\ u_j^2(t) \end{pmatrix} = \begin{pmatrix} \hat{u}_j^0(t) \\ \hat{u}_j^1(t) \\ \hat{u}_j^2(t) \end{pmatrix} e^{i\alpha x_j}, \quad i^2 = -1.$$
 (3.7)

Denote $\hat{\mathbf{u}}_j=(\hat{u}_j^0(t),\hat{u}_j^1(t),\hat{u}_j^2(t))^{\top}$. By substituting Eq. (3.7) into Eq. (3.5), we can obtain

$$(\hat{\mathbf{u}}_j)_t = \widehat{G}(\alpha, h)\hat{\mathbf{u}}_j, \tag{3.8}$$

which $\widehat{G}(\alpha, h)$ is given by

$$\widehat{G}(\alpha, h) = \frac{1}{h^2} ((a - a_1)(Ae^{-i\alpha h} + B + Ce^{i\alpha h}) + a_1(Ae^{-i\alpha h} + B + Ce^{i\alpha h})), \quad (3.9)$$

where the matrices A, B and C are defined in (3.6).

By using (2.7) and (3.8), we can get

$$\hat{\mathbf{u}}_{\mathbf{j}}^{\mathbf{n+1}} = G\hat{\mathbf{u}}_{\mathbf{j}}^{\mathbf{n}},$$

where G is the amplification matrix and is given by

$$G = I + G_{\mathcal{N}} \sum_{l=1}^{5} \hat{b}_{l} M_{l} + G_{\mathcal{L}} \sum_{l=1}^{5} b_{l} M_{l}, \tag{3.10}$$

where

$$M_{1} = I,$$

$$M_{s} = (I - a_{ss}G_{\mathscr{L}})^{-1} \left(I + G_{\mathscr{N}} \sum_{l=1}^{s-1} \hat{a}_{sl} M_{l} + G_{\mathscr{L}} \sum_{l=1}^{s-1} a_{sl} M_{l} \right), \quad 2 \leq s \leq 5,$$

$$G_{\mathscr{L}} = a_{0} a \frac{\tau}{h^{2}} (A e^{-i\alpha h} + B + C e^{i\alpha h}),$$

$$G_{\mathscr{N}} = a (1 - a_{0}) \frac{\tau}{h^{2}} (A e^{-i\alpha h} + B + C e^{i\alpha h}).$$

Due to the complexity of the formula for the amplification matrix G in (3.10), we will try to obtain the threshold value of a_0 numerically. In the following, we briefly show the specific procedure. Note, the amplification matrix G is a function of the variables $\xi, \lambda, a, a_0, \beta_0, \beta_1$. The stability region is defined as a region of the positive real (a_0, λ) -plane such that $|\lambda_G| \leq 1$ according to the Lemma 3.1. However, the spectral radius of the amplification matrix in experiments may be larger than one due to round-off errors. Thus, we relax the condition in Lemma 3.1 by requiring that the spectral radius satisfies $|\lambda_G| \leq 1 + 10^{-10}$. In order to determine the boundary of the stable region, we take $\lambda = 10^\theta$ and $a_0 = 10^\theta$, where the variable θ represents a series of discrete values, each separated by a distance of 0.01, ranging from -10 to 10, for any fixed a, β_0, β_1 and all discrete values of $\xi \in [-\pi, \pi]$. Here, we take $\beta_0 = 2$ and $\beta_1 = 1/12$, which also applies to the second order EIN-DDG scheme. Fig. 1 indicates the stability of the third order EIN-DDG scheme.

We find that the lower bound of the parameter a_0 to ensure the unconditional stability is 0.54 for the third order EIN-DDG scheme. Similarly, we can obtain that the threshold value of a_0 is 0.5 for the second order EIN-DDG scheme. Here, we omit the details.

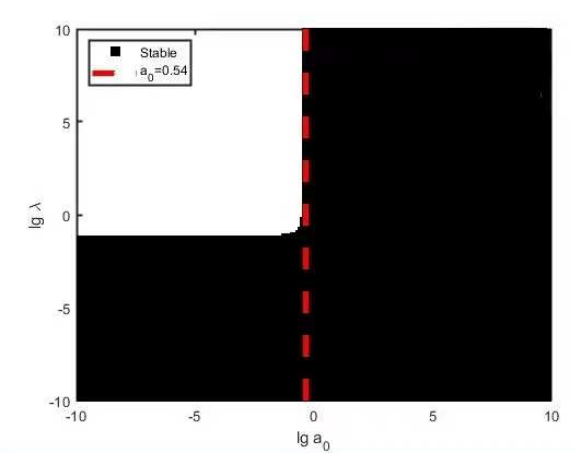


Figure 1: The stability region of the third EIN-DDG scheme corresponds to a_0 and λ for Eq. (2.2). The scheme is stable when a_0 and λ are in the black region.

Remark 3.1. Although our stability analysis is based on a linear model, numerical experiments demonstrate that the above results apply to nonlinear models. We omit details here to save space, see the numerical experiments in Section 4.

Remark 3.2. The above stability results for the one-dimensional case can be extended to the multidimensional case through a similar stability analysis. For 2D numerical results, please refer to Section 4.

Remark 3.3. It should be noted that the threshold for the stabilization parameter a_0 is strongly related to the specific EIN time discretization rather than the spatial discretization method. Therefore, the constant $a_0=0.5$ and $a_0=0.54$ may be invalid if we use other EIN time discretization methods. For example, we cannot obtain the threshold value $a_0=0.5$ and $a_0=0.54$ for our EIN-DDG schemes by using the time discretization in [30].

4. Numerical experiments

In this section, we numerically verify the stability and accuracy orders of the EIN-DDG schemes for both one- and two-dimensional linear and nonlinear equations. Additionally, we compare the computational efficiency of the EX-RK-DDG and EIN-DDG schemes in reaching the steady state for convection-diffusion equations.

For the spatial discretization, we take piecewise constant, linear, and quadratic polynomials for the first order, second order, and third order EIN-DDG schemes, respectively. The equations with periodic boundary conditions are considered unless otherwise specified. We adopt the Lax-Friedrichs numerical flux for the convection part, and take $\beta_0=1$ and $\beta_1=1/12$ for the first order EIN-DDG scheme, and take $\beta_0=2$ and $\beta_1=1/12$ in the numerical flux (2.5) for the second order and third order EIN-DDG schemes.

4.1. The stability and accuracy test

This subsection presents the numerical verification of the stability and the orders of accuracy of the proposed EIN-DDG schemes for linear and nonlinear equations in both one-dimensional and two-dimensional cases. We illustrate the smallest a_0 to assure the stability of the first order, second order, and third order EIN-DDG schemes as 0.5, 0.5, and 0.54, respectively. In this subsection, we take $\tau=h$ and the final time T=1 in all cases unless otherwise stated.

4.1.1. One-dimensional numerical tests

Example 4.1. We consider the one-dimensional diffusion equation

$$\begin{cases} u_t = au_{xx}, & x \in [-\pi, \pi], \\ u(x, 0) = \sin(x) \end{cases}$$

$$\tag{4.1}$$

with the exact solution

$$u(x,t) = e^{-at}\sin(x). (4.2)$$

The L^2 errors and orders of accuracy for this equation with the parameter a=1.0 are listed in Table 1. When $a_0 \ge 0.5$, the first order and second order EIN-DDG schemes

Table 1.	THE L	errors and orde	is or accura	acy for the one	-uimension	iai uiiiusioii eqi	Jation.
Schemes	N	L ² error	Order	L ² error	Order	L ² error	Orde

Schemes	N	L^2 error	Order	L^2 error	Order	L^2 error	Order	
		$a_0 = 0.49$		$a_0 = 0$	$a_0 = 0.5$		$a_0 = 10$	
	320	3.70E - 03	_	3.70E - 03	_	1.11E - 01	-	
	640	1.85E - 03	1.00	1.85E - 03	1.01	5.80E - 02	0.93	
k = 0	1280	9.25E - 04	1.00	9.24E - 04	1.00	2.97E - 02	0.97	
	2560	4.63E - 04	1.00	4.62E - 04	1.00	1.50E - 02	0.98	
	5120	1.77E + 01	-15.23	2.31E - 04	1.00	7.56E - 03	0.99	
		$a_0 = 0.$.49	$a_0 = 0$.5	$a_0 = 10$		
	40	6.61E - 04	_	6.79E - 04	_	1.12E - 01	_	
	80	1.67E - 04	1.99	1.71E - 04	1.99	4.37E - 02	1.36	
k = 1	160	4.39E - 05	1.92	4.28E - 05	2.00	1.44E - 02	1.60	
	320	8.82E - 05	-1.01	1.07E - 05	2.00	4.25E - 03	1.76	
	640	2.83E - 02	-8.33	2.68E - 06	2.00	1.16E - 03	1.88	
		$a_0 = 0.$.53	$a_0 = 0.$	54	$a_0 = 10$		
	40	5.35E - 05	_	3.39E - 05	_	4.35E - 02	_	
	80	1.39E - 05	1.95	4.22E - 06	3.01	1.12E - 02	1.96	
k = 2	160	8.89E - 06	0.64	4.99E - 07	3.08	2.20E - 03	2.35	
	320	4.01E - 05	-2.17	6.44E - 08	2.96	3.58E - 04	2.62	
	640	6.58E - 03	-7.36	8.06E - 09	3.00	5.12E - 05	2.80	

are observed to be stable and achieve optimal orders of accuracy in both space and time. Obviously, these two schemes are unstable for the case of $a_0=0.49$. Additionally, the third order EIN-DDG scheme can obtain optimal orders of accuracy if $a_0\geq 0.54$, whereas the simulation quality deteriorates with mesh refinements if $a_0=0.53$. Note that increasing a_0 results in more significant errors. The simulation results coincide with the theory.

Example 4.2. We compute the viscous Burgers' equation with a source term

$$\begin{cases} u_t + uu_x = au_{xx} + g(x,t), & x \in [-\pi,\pi], \\ u(x,0) = \sin(x), \end{cases}$$
 (4.3)

where $g(x,t)=e^{-2at}\sin(2x)/2$, the exact solution to the equation is given by (4.2). The parameter a is taken as 1.0, and the L^2 errors and orders of the accuracy of the three schemes for Eq. (4.3) are shown in Table 2. Our proposed EIN-DDG schemes can still achieve stability and optimal error accuracy when a_0 exceeds the corresponding threshold. The simulation results for the Eq. (4.3) are similar to those for the Eq. (4.1), and thus are not detailed here.

Fig. 2 shows the L^2 errors of the second order and third order EIN-DDG schemes for solving the viscous Burgers' equation (4.3) with a=1. We take $\tau=0.1$ and T=20.

,							
Schemes	N	L^2 error	Order	L^2 error	Order	L^2 error	Order
		$a_0 = 0.$	49	$a_0 = 0$.5	$a_0 = 10$	
	320	4.15E - 03	_	4.10E - 03	_	1.08E - 01	_
	640	2.07E - 03	1.00	2.04E - 03	1.00	5.68E - 02	0.93
k = 0	1280	1.03E - 03	1.00	1.02E - 03	1.00	2.90E - 02	0.97
	2560	7.03E - 04	0.56	5.09E - 04	1.00	1.47E - 02	0.98
	5120	NaN	NaN	2.55E - 04	1.00	7.39E - 03	0.99
		$a_0 = 0.$	49	$a_0 = 0.5$		$a_0 = 10$	
	40	7.88E - 04	_	7.17E - 04	_	1.11E - 01	_
	80	2.20E - 04	1.84	1.77E - 04	2.02	4.34E - 02	1.36
k = 1	160	1.26E - 04	0.80	4.40E - 05	2.01	1.42E - 02	1.61
	320	6.63E - 04	-2.40	1.10E - 05	2.00	4.20E - 03	1.76
	640	2.06E - 01	-8.28	2.75E - 06	2.00	1.14E - 03	1.88
		$a_0 = 0.$	53	$a_0 = 0.$	54	$a_0 = 1$	0
	40	9.15E - 05	_	4.20E - 05	_	4.31E - 02	_
	80	2.69E - 05	1.77	5.01E - 06	3.07	1.11E - 02	1.96
k = 2	160	1.91E - 05	0.50	5.66E - 07	3.15	2.17E - 03	2.35
	320	8.36E - 05	-2.13	7.35E - 08	2.94	3.53E - 04	2.62

640

1.37E - 02

-7.36

9.20E - 09

3.00

5.04E - 05

2.81

Table 2: The L^2 errors and orders of accuracy for the one-dimensional viscous Burgers' equation.

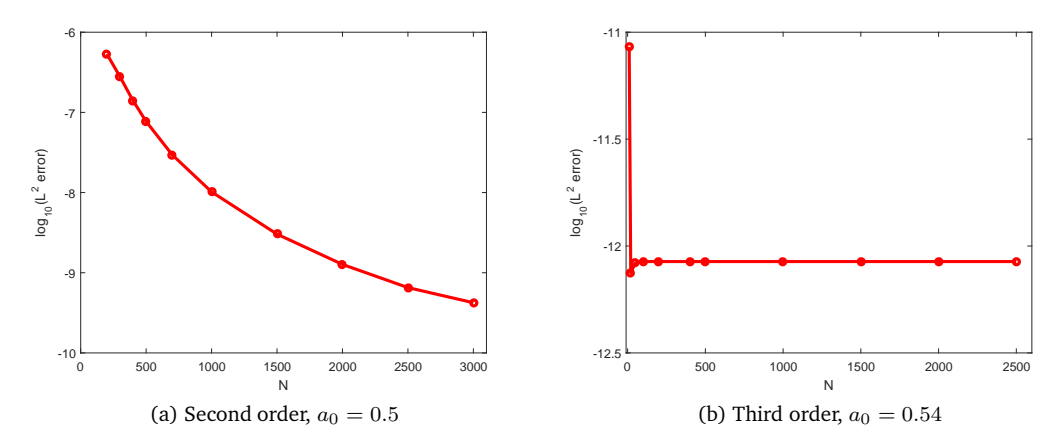


Figure 2: The L^2 errors of the second and third order EIN-DDG schemes for solving (4.3), where a=1, the final time T=20, and time-step is taken as $\tau=0.1$.

As the mesh is refined, the L^2 errors of the second order scheme reach an exponential convergence rate, while the time-step τ remains independent of the mesh size h for the third order scheme.

Example 4.3. We consider the nonlinear convection-diffusion equation

$$\begin{cases} u_t + uu_x = (a(u)u_x)_x + f(x,t), & x \in [-\pi, \pi], \\ u(x,0) = \sin(x), \end{cases}$$
(4.4)

where the diffusion coefficient is $a(u) = u^2 + 2$, the source term is

$$f(x,t) = \frac{1}{4} (4\cos(x+t) + 9\sin(x+t) + 2\sin(2(x+t)) - 3\sin(3(x+t))),$$

and the exact solution of Eq. (4.4) is $u(x,t) = \sin(x+t)$.

In this example, we take a_1 as $a_0 \max_{u^n} \{(u^n)^2 + 2\}$, where u^n is the value of the numerical solution at time level t^n . The numerical results of the three schemes with different a_0 are listed in Table 3. Even though both the convection and diffusion terms are nonlinear, the first order and second order EIN-DDG schemes remain stable and achieve optimal orders of accuracy if $a_1 \geq 0.5 \max_{u^n} \{(u^n)^2 + 2\}$. The third order EIN-DDG scheme is stable and can achieve optimal error accuracy under the condition $a_1 \geq 0.54 \max_{u^n} \{(u^n)^2 + 2\}$. Similarly, the results with $a_0 = 0.49$ and $a_0 = 0.53$ show instability.

4.1.2. Two-dimensional numerical tests

Example 4.4. We consider the two-dimensional diffusion equation

$$u_t = \Delta u, \quad (x, y) \in (-\pi, \pi)^2$$
 (4.5)

Table 3: The L^2 tion.	errors and	orders of accur	acy for the	e one-dimensio	nal nonline	ear convection-	-diffusion equ	ıa-
Schomos	ΔŢ	I ² orror	Order	I ² orror	Ordor	I ² orror	Ordor	

Schemes	N	L^2 error	Order	L^2 error	Order	L^2 error	Order
		$a_0 = 0.49$		$a_0 = 0$	$a_0 = 0.5$.0
	640	1.12E - 02	_	1.14E - 02	_	1.86E - 01	_
	1280	5.62E - 03	1.00	5.71E - 03	1.00	9.65E - 02	0.94
k = 0	2560	2.81E - 03	1.00	2.86E - 03	1.00	4.93E - 02	0.97
	5120	1.41E - 03	1.00	1.43E - 03	1.00	2.49E - 02	0.98
	10240	5.45E - 03	-1.95	7.15E - 04	1.00	1.25E - 02	0.99
		$a_0 = 0.$	49	$a_0 = 0.5$		$a_0 = 10$	
	160	3.66E - 04	_	3.62E - 04	_	9.60E - 02	_
	320	9.54E - 05	1.94	9.47E - 05	1.93	3.44E - 02	1.48
k = 1	640	2.38E - 05	2.00	2.36E - 05	2.01	1.06E - 02	1.70
	1280	8.12E - 06	1.55	5.89E - 06	2.00	2.99E - 03	1.83
	2560	NaN	NaN	1.48E - 06	2.00	7.99E - 04	1.90
		$a_0 = 0.$	53	$a_0 = 0.$	54	$a_0 = 10$	
	320	1.61E - 06	_	1.66E - 06	_	7.26E - 03	_
	640	2.02E - 07	2.99	2.26E - 07	2.88	1.29E - 03	2.49
k = 2	1280	2.55E - 08	2.99	2.85E - 08	2.98	1.98E - 04	2.70
	2560	3.52E - 09	2.86	4.01E - 09	2.83	2.83E - 05	2.81
	5120	NaN	NaN	4.57E - 10	3.13	3.64E - 06	2.96

with the initial condition $u(x,y,0)=\sin(x+y)$. This equation has an exact solution $u(x,y,t)=e^{-2t}\sin(x+y)$. In Table 4, we present a mesh refinement study from 320^2 to 5120^2 grid points to verify the stability of the first order EIN-DDG scheme for the case of $a_0\geq 0.5$, as well as the stability of the second order and third order EIN-DDG schemes when $a_0\geq 0.5$ and $a_0\geq 0.54$, respectively. As expected, the errors for $a_0=10$ are larger, and the numerical order of accuracy converges towards the asymptotic value more slowly with mesh refinements than in the case of $a_0=0.54$.

Example 4.5. We compute the two-dimensional linear convection-diffusion equation

$$u_t + c(u_x + u_y) = a(u_{xx} + u_{yy}), \quad (x, y) \in [-\pi, \pi]^2$$
 (4.6)

with c=a=1, the initial condition $u(x,y,0)=\sin(x+y)$. The equation has an exact solution

$$u(x, y, t) = e^{-2at} \sin(x + y - 2ct).$$

In Table 5, we display the stability and orders of the accuracy of the EIN-DDG schemes for the convection-diffusion equation (4.6) with different a_0 . The simulations of this equation are similar to those of Eq. (4.5) and are therefore not described in detail here.

Table 4: The L^2 errors and orders of accuracy for the two-dimensional diffusion equation.

Schemes	N	L^2 error	Order	L^2 error	Order	L^2 error	Order
		$a_0 = 0.49$		$a_0 = 0$.5	$a_0 = 10$	
	320	1.88E - 03	_	1.88E - 03	_	6.90E - 02	_
	640	9.40E - 04	1.00	9.39E - 04	1.00	3.53E - 02	0.97
k = 0	1280	4.70E - 04	1.00	4.70E - 04	1.00	1.78E - 02	0.99
	2560	2.36E - 04	1.00	2.35E - 04	1.00	8.92E - 03	1.00
	5120	5.26E + 01	-17.77	1.17E - 04	1.00	4.46E - 03	1.00
		$a_0 = 0.$.49	$a_0 = 0.5$		$a_0 = 1$.0
	120	7.38E - 05	_	4.39E - 05	_	2.11E - 02	_
	140	8.04E - 05	-0.56	3.25E - 05	1.96	1.66E - 02	1.55
k = 1	160	8.58E - 05	-0.48	2.49E - 05	1.98	1.35E - 02	1.57
	180	9.56E - 05	-0.92	1.97E - 05	2.01	1.12E - 02	1.57
	200	1.11E - 04	-1.40	1.59E - 05	2.05	9.48E - 03	1.56
		$a_0 = 0.$.53	$a_0 = 0.$	54	$a_0 = 10$	
	120	1.08E - 05	_	2.74E - 06	_	6.29E - 03	_
	140	1.10E - 05	-0.11	1.68E - 06	3.18	4.51E - 03	2.15
k=2	160	1.31E - 05	-1.33	1.15E - 06	2.81	3.36E - 03	2.20
	180	1.35E - 05	-0.24	7.98E - 07	3.13	2.58E - 03	2.24
	200	1.58E - 05	-1.53	5.95E - 07	2.79	2.04E - 03	2.25

Table 5: The L^2 errors and orders of accuracy for the two-dimensional linear convection-diffusion equation.

Schemes	N	L^2 error	Order	L^2 error	Order	L^2 error	Order
		$a_0 = 0.49$		$a_0 = 0$	$a_0 = 0.5$.0
	160	1.24E - 02	_	1.23E - 02	_	1.70E - 01	_
	320	6.11E - 03	1.02	6.06E - 03	1.02	9.39E - 02	0.86
k = 0	640	3.02E - 03	1.01	3.00E - 03	1.02	4.85E - 02	0.95
	1280	1.50E - 03	1.01	1.49E - 03	1.01	2.45E - 02	0.99
	2560	2.56E - 02	-4.09	7.44E - 04	1.00	1.23E - 02	1.00
		$a_0 = 0.$	49	$a_0 = 0.5$		$a_0 = 10$	
	120	1.03E - 03	_	5.90E - 04	_	3.10E - 02	_
	140	9.98E - 04	0.20	4.28E - 04	2.08	2.43E - 02	1.58
k = 1	160	9.68E - 04	0.23	3.24E - 04	2.09	1.96E - 02	1.59
	180	9.93E - 04	-0.22	2.54E - 04	2.06	1.63E - 02	1.59
	200	1.07E - 03	-0.71	2.05E - 04	2.02	1.38E - 02	1.58
		$a_0 = 0.$	53	$a_0 = 0.$	54	$a_0 = 1$.0
	120	6.08E - 05	_	2.28E - 05	_	9.21E - 03	_
	140	4.58E - 05	1.84	1.39E - 05	3.22	6.59E - 03	2.17
k=2	160	6.83E - 05	-2.99	9.30E - 06	3.00	4.90E - 03	2.22
	180	6.47E - 05	0.46	6.48E - 06	3.07	3.76E - 03	2.25
	200	6.89E - 05	-0.60	4.77E - 06	2.90	2.96E - 03	2.26

Example 4.6. We consider the two-dimensional viscous Burgers' equation with a source term

$$u_t + \frac{1}{2}((u^2)_x + (u^2)_y) = a(u_{xx} + u_{yy}) + f(x, y, t), \quad (x, y) \in [-\pi, \pi]^2$$
 (4.7)

with

$$a = 1$$
, $f(x, y, t) = e^{-4at} \sin(2(x+y))$,

the initial condition $u(x, y, 0) = \sin(x + y)$, and the exact solution

$$u(x, y, t) = e^{-2at} \sin(x + y).$$

Table 6 shows that the first order and second order EIN-DDG schemes achieve optimal accuracy when $a_0 \ge 0.5$, whereas the results degrade significantly if $a_0 = 0.49$. For the third order EIN-DDG scheme, the stability threshold for a_0 is 0.54. Additionally, a more extensive a_0 leads to significantly greater errors.

Example 4.7. We solve the two-dimensional nonlinear convection-diffusion equation

$$u_t + \frac{1}{2} ((u^2)_x + (u^2)_y) = \nabla \cdot (a(u)\nabla u) + f(x, y, t), \quad (x, y) \in (-\pi, \pi)^2,$$
 (4.8)

Table 6: The L^2 errors and orders of accuracy for the two-dimensional Burgers' equation.

	N	L^2 error	Order	L^2 error	Order	L^2 error	Order
		$a_0 = 0.$.49	$a_0 = 0$.5	$a_0 = 1$	0
	160	3.64E - 03	_	3.64E - 03	_	1.27E - 01	_
	320	1.82E - 03	1.00	1.82E - 03	1.00	6.70E - 02	0.92
k = 0	640	9.13E - 04	1.00	9.12E - 04	1.00	3.49E - 02	0.94
	1280	4.57E - 04	1.00	4.56E - 04	1.00	1.76E - 02	0.99
	2560	7.41E - 02	-7.34	2.28E - 04	1.00	8.81E - 03	1.00
		$a_0 = 0.49$		$a_0 = 0$.5	$a_0 = 10$	
	120	1.24E - 04	_	4.65E - 05	_	2.08E - 02	_
	140	1.40E - 04	-0.79	3.47E - 05	1.90	1.64E - 02	1.56
k = 1	160	1.54E - 04	-0.72	2.70E - 05	1.87	1.33E - 02	1.56
	180	1.92E - 04	-1.87	2.14E - 05	1.98	1.10E - 02	1.57
	200	2.02E - 04	-0.48	1.69E - 05	2.22	9.36E - 03	1.57
		$a_0 = 0.$.53	$a_0 = 0.$	54	$a_0 = 10$	
	120	1.30E - 05	_	2.96E - 06	_	6.19E - 03	_
	140	1.86E - 05	-2.33	1.84E - 06	3.11	4.44E - 03	2.15
k = 2	160	7.42E - 05	-10.35	1.24E - 06	2.95	3.31E - 03	2.21
	180	9.29E - 05	-1.91	8.60E - 07	3.09	2.54E - 03	2.24
	200	9.89E - 05	-0.59	6.16E - 07	3.17	2.00E - 03	2.25

Table 7: The L^2 errors and orders of accuracy for the two-dimensional nonlinear convection-diffusion equation.

Schemes	N	L^2 error	Order	L^2 error	Order	L^2 error	Order
		$a_0 = 0.49$		$a_0 = 0$.5	$a_0 = 10$	
	160	7.45E - 03	_	7.68E - 03	_	2.05E - 01	_
	320	3.76E - 03	0.99	3.88E - 03	0.99	1.20E - 01	0.77
k = 0	640	1.88E - 03	1.00	1.94E - 03	1.00	6.44E - 02	0.90
	1280	9.43E - 04	1.00	9.73E - 04	1.00	3.30E - 02	0.96
	2560	4.72E - 04	1.00	4.87E - 04	1.00	1.67E - 02	0.99
		$a_0 = 0.$	49	$a_0 = 0.5$		$a_0 = 10$	
	40	1.08E - 03	_	1.10E - 03	_	1.70E - 01	_
	80	2.59E - 04	2.07	2.63E - 04	2.07	8.74E - 02	0.96
k = 1	160	6.41E - 05	2.01	6.51E - 05	2.01	3.69E - 02	1.24
	320	1.63E - 05	1.98	1.66E - 05	1.98	1.36E - 02	1.44
	640	4.06E - 06	2.00	4.13E - 06	2.00	4.35E - 03	1.64
		$a_0 = 0.$	53	$a_0 = 0.$	54	$a_0 = 10$	
	40	1.26E - 04	_	1.29E - 04	_	1.03E - 01	_
	80	1.76E - 05	2.83	1.81E - 05	2.83	4.35E - 02	1.24
k = 2	160	2.34E - 06	2.92	2.39E - 06	2.92	1.40E - 02	1.63
	320	3.04E - 07	2.94	3.10E - 07	2.95	3.50E - 03	2.00
	640	4.10E - 08	2.89	3.94E - 08	2.98	6.75E - 04	2.37

where the diffusion coefficient $a(u) = u^2 + 1$, the initial condition $u(x, y, 0) = \sin(x + y)$, the exact solution is $u(x, y, t) = e^{-2t} \sin(x + y)$, and the source term

$$f(x,y,t) = e^{-6t} \left(-1 + 2e^{2t} \cos(x+y) - 3\cos(2(x+y)) \right) \sin(x+y).$$

We take the stabilization parameter as $a_1 = a_0 \max_{u^n} \{(u^n)^2 + 1\}$. In Table 7, we display the numerical results for our proposed schemes, which present the optimal orders of accuracy of $a_0 = 0.5$ and $a_0 = 0.54$ for the first order, second order, and third order EIN-DDG scheme. In addition, this table shows the slow progress of the numerical orders of accuracy towards the asymptotic value for the case of $a_0 = 10$. However, the proposed schemes still show stable performance for this equation when $a_0 = 0.49$ and $a_0 = 0.53$ due to the meshes not being refined enough.

4.2. Computational efficiency

In this subsection, we compare the computational efficiency of the third order EX-RK-DDG and EIN-DDG schemes in reaching the steady state for one- and two-dimensional convection-diffusion equations to demonstrate the advantages of our proposed methods. In the following examples, the steady state is assumed to be achieved when the residual is less than 10^{-10} .

Example 4.8. We solver the one-dimensional linear convection-diffusion equation

$$\begin{cases} u_t + cu_x = au_{xx}, & x \in [0, 1], \\ u(0) = 1, & u(1) = 2 \end{cases}$$
(4.9)

with c = 1, a = 0.01. The initial condition is

$$u(x,0) = 1 + e^{-\frac{c}{a}(1-x)}.$$

Example 4.9. Here, we consider the linear convection-diffusion equation with a source term

$$\begin{cases} u_t + u_x = au_{xx} + a\pi^2 \sin(\pi x) + \pi \cos(\pi x), & x \in [0, 1], \\ u(0) = 0, & u(1) = 1 \end{cases}$$
 (4.10)

with a = 0.01, the initial condition is

$$u(x,0) = \sin(\pi x) + \frac{e^{\frac{x}{a}} - 1}{e^{\frac{1}{a}} - 1}.$$

Example 4.10. In this example, we consider the following viscous Burgers' equation:

$$u_t + \left(\frac{1}{2}u^2\right)_x = au_{xx},\tag{4.11}$$

augmented with a=0.01, the boundary condition is u(0)=1.0, u(1)=2.0, and the initial condition is determined by

$$u(x,0) = \frac{2}{1 - e^{-\frac{1}{a}(1-x)}/3} - 1.$$

Example 4.11. We solve the one-dimensional viscous Burgers' equation with a source term

$$\begin{cases} u_t + u_x u = a u_{xx} + f(x) & \text{in } \Omega = [-1, 1], \\ u(\pm 1) = 0, \end{cases}$$
 (4.12)

where a = 0.01, the initial condition is

$$u(x,0) = \sin(\pi x), \quad f(x) = a\pi^2 \sin(\pi x) + \pi \cos(\pi x) \sin(\pi x).$$

Example 4.12. Next, we consider the convection-diffusion equation in two-dimension

$$u_t + u_x = a(u_{xx} + u_{yy}), \quad 0 \le x, y \le 1$$
 (4.13)

with a = 0.01, the initial condition is

$$u(x,y,0) = \frac{1}{\sinh \sigma} e^{\frac{x}{2a}} \sin(\pi y) \left[2e^{-\frac{1}{2a}} \sinh(\sigma x) + \sinh \sigma (1-x) \right],$$

where $\sigma^2=\pi^2+0.25/a^2$. The initial condition gives the boundary conditions for this equation.

Example 4.13. We solver the two-dimensional convection-diffusion equation with a source term

$$u_t + u_x + u_y = a(u_{xx} + u_{yy}) - \frac{1}{a} 6e^{-\frac{x^6 + y^6}{a}}$$

$$\times \left(x^5 + 6x^{10} + y^4(y + 6y^6 - 5a) - 5x^4a\right), \quad 0 \le x, y \le 1,$$
(4.14)

where a = 0.01, the initial condition is

$$u(x, y, 0) = e^{-\frac{x^6 + y^6}{a}}.$$

The initial condition gives the boundary conditions for this equation.

Tables 8-13 show the maximum time-steps $\tau_{\rm max}$, the number of time-steps nt, the numerical steady time t, and the CPU time to reach the steady state for the Eqs. (4.9)-(4.14). These tables demonstrate that our third order EIN-DDG scheme permits a considerably larger time-step than the third order EX-RK-DDG scheme, thereby reducing

Table 8: The maximum time-steps $au_{
m max}$, the number of time-steps nt, the numerical steady time t, and the CPU time required to reach the steady state for third order EX-RK-DDG scheme and EIN-DDG scheme for the Eq. (4.9) with $N=200,\ c=1$ and a=0.01.

	a_0	$ au_{ m max}$	nt	t	CPU time (s)
3rd order EX-RK-DDG	_	9.65E-05	7,554	0.7290	14.752
	1.2	0.0450	448	20.1600	2.607
3rd order EIN-DDG	1.5	0.0495	1,377	68.1615	7.939
	2.0	0.0540	1,640	88.5600	10.016

Table 9: The maximum time-steps $\tau_{\rm max}$, the number of time-steps nt, the numerical steady time t, and the CPU time required to reach the steady state for third order EX-RK-DDG scheme and EIN-DDG scheme for the Eq. (4.10) with N=200 and a=0.01.

	a_0	$ au_{ m max}$	nt	t	CPU time (s)
3rd order EX-RK-DDG	_	9.55E-05	18,135	1.7319	31.361
	1.2	0.0455	1,124	51.1420	6.210
3rd order EIN-DDG	1.5	0.0497	2,620	130.2140	14.809
	2.0	0.0543	3,021	163.8890	18.572

Table 10: The maximum time-steps $\tau_{\rm max}$, the number of time-steps nt, the numerical steady time t, and the CPU time required to reach the steady state for third order EX-RK-DDG scheme and EIN-DDG scheme for the Eq. (4.11) with N=200 and a=0.01.

	a_0	$ au_{ m max}$	nt	t	CPU time (s)
3rd order EX-RK-DDG	_	9.38E-05	6,739	0.6318	14.490
	1.2	0.0455	440	20.0200	2.585
3rd order EIN-DDG	1.5	0.0500	1,418	70.9000	7.219
	2.0	0.0535	1,154	61.7390	6.796

Table 11: The maximum time-steps $\tau_{\rm max}$, the number of time-steps nt, the numerical steady time t, and the CPU time required to reach the steady state for third order EX-RK-DDG scheme and EIN-DDG scheme for the Eq. (4.12) with N=200 and a=0.01.

	a_0	$ au_{ m max}$	nt	t	CPU time (s)
3rd order EX-RK-DDG	_	3.64E-04	11,147	4.0575	25.816
	1.2	0.0475	105	4.9875	0.688
3rd order EIN-DDG	1.5	0.0525	228	11.9700	1.421
	2.0	0.0583	1,248	72.7584	5.430

Table 12: The maximum time-steps $\tau_{\rm max}$, the number of time-steps nt, the numerical steady time t, and the CPU time required to reach the steady state for third order EX-RK-DDG scheme and EIN-DDG scheme for the Eq. (4.13) with N=100 and a=0.01.

	a_0	$ au_{ m max}$	nt	t	CPU time (s)
3rd order EX-RK-DDG	_	3.15E-04	5,338	1.6815	2537.570
3rd order EIN-DDG	1.2	0.0430	353	15.1790	636.299
	1.5	0.0475	432	20.5200	834.667
	2.0	0.0505	301	15.2005	583.315

Table 13: The maximum time-steps $\tau_{\rm max}$, the number of time-steps nt, the numerical steady time t, and the CPU time required to reach the steady state for third order EX-RK-DDG scheme and EIN-DDG scheme for the Eq. (4.14) with N=100 and a=0.01.

	a_0	$ au_{ m max}$	nt	t	CPU time (s)
3rd order EX-RK-DDG	_	3.00E-04	6,267	1.8801	2401.780
3rd order EIN-DDG	1.2	0.0210	135	2.8350	263.433
	1.5	0.0240	428	10.2720	794.163
	2.0	0.0260	304	7.9040	533.847

CPU time. For example, Tables 8 and 9 show that the computational time of the third order EIN-DDG scheme with $a_0 = 1.5$ is reduced by 46.2% and 52.8%, respectively, compared to the third order EX-RK-DDG scheme. Furthermore, when $a_0 = 2.0$, Tables 12 and 13 indicate that the CPU time of the third order EIN-DDG scheme can decrease by 77.0% and 77.8%, respectively, in contrast with the third order EX-RK-DDG scheme for the two-dimensional equations (4.13) and (4.14). These results demonstrate the high computational efficiency of the proposed methods.

5. Concluding remarks

We have developed the DDG method coupled with the EIN time-marching methods for diffusion equations and convection-diffusion equations in both one- and two-dimensional cases. We have demonstrated that the schemes are stable with a relaxed time-step restriction and an appropriate stabilization parameter a_0 . To verify the va-

lidity of our proposed method, we tested some numerical experiments, including one-dimensional and two-dimensional linear and nonlinear equations. The numerical results show that the first order and second order EIN-DDG schemes are stable and can obtain the optimal orders of accuracy if $a_0 \geq 0.5$, and the third order EIN-DDG scheme holds when $a_0 \geq 0.54$. We also presented the computational efficiency of the EX-RK-DDG and EIN-DDG schemes for reaching the steady state in convection-diffusion equations, demonstrating the effectiveness of our EIN-DDG scheme. In the future, we will explore the application of the EIN-DDG scheme for equations with non-periodic boundary conditions and non-uniform meshes.

Acknowledgments

This work is supported by the Postgraduate Scientific Research Innovation Project of Xiangtan University (No. XDCX2023Y134), by the National Natural Science Foundation of China Project (Nos. 12071402, 12261131501), by the Project of Scientific Research Fund of the Hunan Provincial Science and Technology Department (Nos. 2022RC3022, 2023GK2029, 2024ZL5017, 2024JJ1008), and by the Program for Science and Technology Innovative Research Team in Higher Educational Institutions of Hunan Province of China, and the high-performance computing resources provided by the School of Mathematical Sciences of Beihang University.

References

- [1] U. ASCHER, S. RUUTH, AND R. SPITERI, *Implicit-explicit Runge-Kutta methods for time-dependent partial differential equations*, Appl. Numer. Math. 25 (1997), 151–167.
- [2] M. CALVO, J. DE FRUTOS, AND J. NOVO, *Linearly implicit Runge-Kutta methods for advection-reaction-diffusion equations*, Appl. Numer. Math. 37 (2001), 535–549.
- [3] W. CAO, H. LIU, AND Z. ZHANG, Superconvergence of the direct discontinuous Galerkin method for convection-diffusion equations, Numer. Methods Partial Differ. Equ. 33 (2017), 290–317.
- [4] J. Cheng, X. Yang, X. Liu, T. Liu, and H. Luo, A direct discontinuous Galerkin method for the compressible Navier-Stokes equations on arbitrary grids, J. Comput. Phys. 327 (2016), 484–502.
- [5] G. COOPER AND A. SAYFY, Additive Runge-Kutta methods for stiff ordinary differential equations, Math. Comput. 40 (1983), 207–218.
- [6] M. Q. DE LUNA AND D. I. KETCHESON, Maximum principle preserving space and time flux limiting for diagonally implicit Runge-Kutta discretizations of scalar convection-diffusion equations, J. Sci. Comput. 92 (2022), p. 102.
- [7] J. DOUGLAS JR. AND T. DUPONT, *Alternating-direction Galerkin methods on rectangles*, in: Numerical Solution of Partial Differential Equations II, Academic Press, (1971), 133–214.
- [8] Y. Du and J. Ekaterinaris, On the stability and CPU time of the implicit Runge-Kutta schemes for steady state simulations, Commun. Comput. Phys. 20 (2016), 486–511.
- [9] L. Duchemin and J. Eggers, *The explicit-implicit-null method: Removing the numerical instability of PDEs*, J. Comput. Phys. 263 (2014), 37–52.

- [10] J. EGGERS, J. LISTER, AND H. STONE, Coalescence of liquid drops, J. Fluid. Mech. 401 (1999), 293–310.
- [11] F. Filbet and S. Jin, A class of asymptotic-preserving schemes for kinetic equations and related problems with stiff sources, J. Comput. Phys. 229 (2010), 7625–7648.
- [12] J. Frank, W. Hundsdorfer, and J. Verwer, *On the stability of implicit-explicit linear multistep methods*, Appl. Numer. Math. 25 (1997), 193–205.
- [13] J. GEISER, Iterative operator-splitting methods with higher-order time integration methods and applications for parabolic partial differential equations, J. Comput. Appl. Math. 217 (2008), 227–242.
- [14] E. HAIRER AND G. WANNER, Solving Ordinary Differential Equations II, Springer-Verlag, 1996.
- [15] A. JAUST AND J. SCHÜTZ, A temporally adaptive hybridized discontinuous Galerkin method for time-dependent compressible flows, Comput. & Fluids 98 (2014), 177–185.
- [16] L. JAY, Inexact simplified Newton iterations for implicit Runge-Kutta methods, SIAM J. Numer. Anal. 38 (2000), 1369–1388.
- [17] V. KAZEMI-KAMYAB, A. H. VAN ZUIJLEN, AND H. BIJL, Analysis and application of high order implicit Runge-Kutta schemes to collocated finite volume discretization of the incompressible Navier-Stokes equations, Comput. & Fluids, 108 (2015), 107–115.
- [18] N. Lei, J. Cheng, and C.-W. Shu, High order conservative Lagrangian schemes for twodimensional radiation hydrodynamics equations in the equilibrium-diffusion limit, J. Comput. Phys. 503 (2024), p. 112840.
- [19] H. LIU, Optimal error estimates of the direct discontinuous Galerkin method for convection-diffusion equations, Math. Comput. 84 (2015), 2263–2295.
- [20] H. LIU AND H. WEN, Error estimates of the third order Runge-Kutta alternating evolution discontinuous Galerkin method for convection-diffusion problems, ESAIM Math. Model. Numer. Anal. 52 (2018), 1709–1732.
- [21] H. LIU AND J. YAN, The direct discontinuous Galerkin (DDG) methods for diffusion problems, SIAM J. Numer. Anal. 47 (2009), 675–698.
- [22] H. LIU AND J. YAN, The direct discontinuous Galerkin (DDG) method for diffusion with interface corrections, Commun. Comput. Phys. 8 (2010), 541–564.
- [23] L. PARESCHI AND G. RUSSO, *Implicit-explicit Runge-Kutta schemes and applications to hyperbolic systems with relaxation*, J. Sci. Comput. 25 (2005), 129–155.
- [24] S. J. RUUTH, *Implicit-Explicit Methods for Time-Dependent PDE's*, PhD Thesis, University of British Columbia, 1993.
- [25] H. Shi and Y. Li, Local discontinuous Galerkin methods with implicit-explicit multistep time-marching for solving the nonlinear Cahn-Hilliard equation, J. Comput. Phys. 394 (2019), 719–731.
- [26] P. SMEREKA, Semi-implicit level set methods for curvature and surface diffusion motion, J. Sci. Comput. 19 (2003), 439–456.
- [27] M. TAN, J. CHENG, AND C.-W. SHU, Stability of high order finite difference and local discontinuous Galerkin schemes with explicit-implicit-null time-marching for high order dissipative and dispersive equations, J. Comput. Phys. (2022), p. 111314.
- [28] M. TAN, J. CHENG, AND C.-W. SHU, Stability of spectral collocation schemes with explicit-implicit-null time-marching for convection diffusion and convection-dispersion equations, East Asian J. Appl. Math. 13 (2023), 464–498.
- [29] C. VIDDEN AND J. YAN, Direct discontinuous Galerkin method for diffusion problems with symmetric structure, J. Comput. Math. 31 (2013), 638–662.
- [30] H. WANG AND Q. ZHANG, The direct discontinuous Galerkin methods with implicit-explicit

- *Runge-Kutta time marching for linear convection-diffusion problems*, Commun. Appl. Math. Comput. 4 (2022), 271–292.
- [31] H. Wang, Q. Zhang, S. Wang, and C.-W. Shu, Local discontinuous Galerkin methods with explicit-implicit-null time discretizations for solving nonlinear diffusion problems, Sci. China. Math. 63 (2020), 183–204.
- [32] C. Xu and T. Tang, Stability analysis of large time-stepping methods for epitaxial growth models, SIAM J. Numer. Anal. 44 (2006), 1759–1779.
- [33] J. YAN, A new nonsymmetric discontinuous Galerkin method for time dependent convection diffusion equations, J. Sci. Comput. 54 (2013), 663–683.
- [34] X. Yang, J. Cheng, H. Luo, and Q. Zhao, A reconstructed direct discontinuous Galerkin method for simulating the compressible laminar and turbulent flows on hybrid grids, Comput. & Fluids 168 (2018), 216–231.
- [35] X. Yang, J. Cheng, H. Luo, and Q. Zhao, Robust implicit direct discontinuous Galerkin method for simulating the compressible turbulent flows, AIAA J. 57 (2019), 1113–1132.
- [36] N. YI, Y. HUANG, AND H. LIU, A direct discontinuous Galerkin method for the generalized Korteweg-de Vries equation: Energy conservation and boundary effect, J. Comput. Phys. 242 (2013), 351–366.
- [37] H. Yue, J. Cheng, and T. Liu, A symmetric direct discontinuous Galerkin method for the compressible Navier-Stokes equations, Commun. Comput. Phys. 22 (2017), 375–392.
- [38] F. ZHANG, J. CHENG, AND T. LIU, A direct discontinuous Galerkin method for the incompressible Navier-Stokes equations on arbitrary grids, J. Comput. Phys. 380 (2019), 269–294.
- [39] J. Zhu, L. Chen, J. Shen, and V. Tikare, Coarsening kinetics from a variable-mobility Cahn-Hilliard equation: Application of a semi-implicit Fourier spectral method, Phys. Rev. E. 60 (1999), 3564–3572.